

Aminoacyl and Peptidyl Analogs of Chloramphenicol as Slow-Binding Inhibitors of Ribosomal Peptidyltransferase: A New Approach for Evaluating Their Potency

MARIA MICHELINAKI, PETROS MAMOS, CHARALAMBOS COUTSOGEORGOPOULOS, and DIMITRIOS L. KALPAXIS

Laboratory of Biochemistry, School of Medicine, University of Patras, 261 10 Patras, Greece

Received July 8, 1996; Accepted September 20, 1996

SUMMARY

In a model system derived from *Escherichia coli*, acetylphenylalanyl-puromycin is produced in a pseudo-first-order reaction between the preformed acetylphenylalanyl/tRNA/poly(U)/ribosome complex (complex C) and excess puromycin. Two aminoacyl analogs [**3**, Gly-chloramphenicol (CAM); **4**, L-Phe-CAM] and two peptidyl analogs (**2**, L-Phe-Gly-CAM; **5**, Gly-Phe-CAM) of CAM (**1**) were tested as inhibitors in this reaction. Detailed kinetic analysis suggests that these analogs (**I**) react competitively with complex C and form the complex C*I, which is inactive toward puromycin. C*I is formed via a two-step mechanism in which C*I is the product of a slow conformational change of the initial encounter complex CI according to the equation $C + I \rightleftharpoons CI \rightleftharpoons C^*I$. Furthermore, we provide evidence that analog **5** may react further with C*I forming the species

C*I₂. The values of the apparent association rate constant (k_{assoc}) are $1.45 \times 10^4 \text{ M}^{-1} \text{ sec}^{-1}$ for **2**, $5.5 \times 10^3 \text{ M}^{-1} \text{ sec}^{-1}$ for **3**, and $1.8 \times 10^3 \text{ M}^{-1} \text{ sec}^{-1}$ for **4**. In the case of analog **5**, k_{assoc} is a linear function of the inhibitor concentration; when $[I]$ approaches zero, the k_{assoc} value is equal to $3.8 \times 10^2 \text{ M}^{-1} \text{ sec}^{-1}$. Such values allow the classification of CAM analogs as slow-binding inhibitors. According to k_{assoc} values, we could surmise that analog **2** is 2.5-fold more potent than **3** and 8-fold more potent than **4**. The relative potency of analog **5** is the lowest among the analogs and is dependent on its concentration. The results are compared with previous data and discussed on the basis of a possible retro-inverso relationship between CAM analogs and puromycin.

CAM inhibits ribosomal protein synthesis in prokaryotes as measured by various *in vitro* and *in vivo* assays (1, 2). This antibiotic behaves as an inactive analog of the acceptor substrate and after binding to the peptidyltransferase (EC 2.3.2.12) center, it interferes competitively with the interaction of true substrates (3–6). However, there also is evidence for a noncompetitive (7) or a mixed noncompetitive (8) mode of CAM inhibition. It is possible that the bound antibiotic somehow induces a conformational change in the rRNA, which results in modification of the peptidyltransferase catalytic rate constant (8).

Many reports have accumulated in an attempt to interpret the inhibitory properties of CAM on a molecular basis. A unique opportunity for these studies was afforded by the fact that in cell-free systems, puromycin can be used as a substitute of the 3' terminus of aminoacyl-tRNA and can form peptide bonds between its free amino group and the carboxyl terminus of appropriate model peptidyl-tRNAs (2). However, attempts to define the exact structural relationship between CAM and the 3'-end of the aminoacyl-tRNA or puromycin

have never been successful (2). In the direction of other explanations, a theoretical study (9) relates CAM to a peptide backbone in peptidyl-tRNA bound to the P-site and to the corresponding transition state involving aminoacyl-tRNA and a catalytic center on the ribosome. The validity of this suggestion has been widely argued because CAM is regarded essentially as an A-site inhibitor. In another study, Bhuta *et al.* (10) suggested that CAM resembles a transition state for the puromycin reaction and proposed that the biological activity of CAM can be explained in terms of retro-inverso relationship.

Despite the fact that much has been accomplished, there remains great interest in the elucidation of the CAM mechanism of action on protein synthesis (3–6, 11–14). A valuable tool for exploring these new aspects could be the use of aminoacyl and peptidyl analogs of CAM. Previous investigations (15–17) concerning synthetic derivatives of CAM, in which the dichloroacetyl group has been replaced by aminoacyl or peptidyl groups, revealed that this substitution has a prominent influence on the activity of CAM. On the assumption that these analogs behave as classic competitive inhibitors, their potency has been expressed on the basis of K_i alone (17). Despite this seemingly satisfactory one-site modeling, it

This work was supported in part by a grant from the General Secretariat of Research and Technology, Ministry of Development of Greece.

is evident from the kinetic analysis of Drainas *et al.* (17) that the assumption of classical competitive inhibition may not be sufficient to express the overall inhibitory effect. Therefore, parameters in addition to K_i are needed for full characterization of potency. In view of the above observations, we thought that it was interesting to examine further an available series of aminoacyl analogs of CAM (17) as well as the peptidyl analog **5** (Fig. 1) through detailed kinetic analysis. A better understanding of the kinetic mechanism involved in peptidyltransferase inhibition will have an impact not only on basic research but also in clinical practice. The results that we present demonstrate that the simple equilibrium $C + I \rightleftharpoons CI$ may express only the initial encounter between the ribosomal complex (C) and the inhibitor (I). Subsequently, as a result of conformational changes, a slow isomerization occurs ($CI \rightleftharpoons C^*I$), which requires the use of constants in addition to K_i . An explanation of the differential influence of the acylamino side-chain substitution on CAM kinetic behavior is also presented.

Experimental Procedures

Materials. Poly(U), GTP (disodium salt), ATP (disodium salt), phenylalanine, puromycin dihydrochloride, and heterogeneous tRNA from *Escherichia coli* strain W were obtained from Sigma Chemical (St. Louis, MO). L-Phenyl-[2,3-³H]alanine was purchased from Amersham (Arlington Heights, IL). Cellulose nitrate filters (type HA, 24-nm diameter, 0.45- μ m pore size) were from Millipore (Bedford, MA). Spiramycin was a mixture of spiramycins I, II, and III (Sigma Chemical). CAM free base [D-(-)-*threo*-1-(*p*-nitrophenyl)-2-amino-1,3-propanediol] (**1**) was also from Sigma Chemical. Tritylglycin was synthesized according to known methods (18, 19). *N*-Hydroxysuccinimide ester of tritylglycyl-L-phenylalanine was prepared in 65% yield from tritylglycyl-L-phenylalanine according to Anderson *et al.* (20). Analogs **2–4** (Fig. 1) were synthesized as described previously (17).

Preparation of D-(-)-*threo*-1-(*p*-Nitrophenyl)-2-(glycyl-L-phenylalanyl-amido)-1,3-propanediol (Analog **5**)

Preparation of D-(-)-*threo*-1-(*p*-nitrophenyl)-2-(*N*-tritylglycyl-L-phenylalanyl-amido)-1,3-propanediol (analog **5a).** A solution of **1** (2.33 g, 11 mmol) in dry dimethylformamide (10 ml) and triethylamine (2 ml) was cooled at 0°. Hydroxysuccinimide ester of tritylglycyl-L-phenylalanine (5.62 g, 10 mmol) was added to the above solution with stirring. The mixture was incubated for 20 min at 0° and then at room temperature overnight with continuous stirring. The resulting solution was partitioned between 10 ml of a saturated solution of sodium chloride and 70 ml of ethyl acetate. The ethyl acetate layer was extracted twice with 10 ml of 5% citric acid, once with 10 ml of 10% sodium carbonate, and with 10 ml of saturated solution of sodium chloride. The ethyl acetate layer was then dried over MgSO₄ and evaporated *in vacuo*. The resulting light-yellow powder was recrystallized from ethyl acetate and yielded 5.51 g (83.67%) of white crystals. Because the product contained a small portion of impurities, as shown by TLC, the product was further purified on a silica gel column (120 g, elution with CH₂Cl₂/CH₃OH, from 98:2 to 97:3). The final yield was 4.8 g (72.9%); TLC (in chloroform/methanol, 9:1) R_F = 0.77.

Preparation of the tosylate of dipeptidyl analog of CAM (analog **5b).** An amount of **5a** (4.61 g, 7 mmol) was dissolved in 25 ml of a warm (60°) solution of 10 mmol of toluene-4-sulfonic acid monohydrate in isopropyl alcohol. The mixture was further incubated at 60° for 5 min and then the tosylate was crystallized by letting the mixture stand at room temperature overnight. The white crystals were filtered under vacuum, washed with small aliquots of ether, and recrystallized from isopropyl alcohol. The yield was 3.25 g

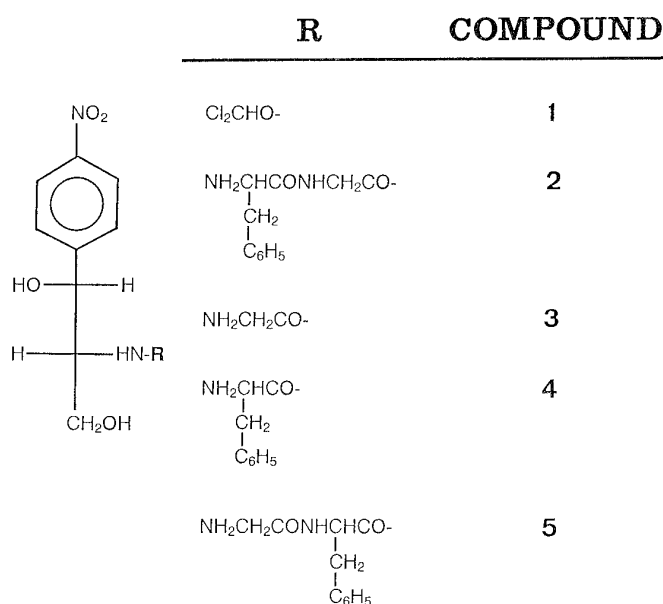


Fig. 1. Structures of CAM and its analogs.

(78.8%) [m.p. = 232–233°; TLC (in butanol/acetic acid/water, 2:3:5) R_F = 0.74].

Preparation of dipeptidyl analog of CAM. Compound **5b** was obtained as free base from its tosylate. Then, 3 mmol (1.77 g) of **5b** was partitioned between 50 ml of ethyl acetate and 8 ml of 10% sodium carbonate. The ethyl acetate layer was extracted three times with 10 ml of a saturated solution of sodium chloride, dried over MgSO₄, and evaporated *in vacuo*. The yield was 479.6 mg (38.3%); TLC (in butanol/acetic acid/water, 2:3:5) R_F = 0.74; UV_{max} (2% CH₃COOH) = 279 nm (ϵ = 4040); MS (FAB) m/z 417 (M + H). Elemental analysis gave the following data: C, 57.59; H, 5.72; N, 13.60.

Biochemical preparations

Salt-washed ribosomes (0.5 M NH₄Cl) and factors washable from ribosomes were obtained from frozen *E. coli* B cells as described previously (21). Complex C was prepared and purified through adsorption on cellulose nitrate filters, as reported previously (21). The adsorbed radioactivity was measured in a liquid scintillation spectrometer. Controls without poly(U) were included in each experiment, and the values obtained were subtracted.

Puromycin Reaction and First-Order Analysis

The puromycin reaction was carried out at 25°, as described previously (22). In the absence of inhibitor, the reaction follows pseudo-first-order kinetics to >80% depletion of complex C at all concentrations of puromycin that were used. The relationships $\ln[100/(100 - x')] = k_{obs} \times t$ and $k_{obs} = k_3[S]/(K_s + [S])$ hold, and the values of k_3 and K_s can be obtained from the double-reciprocal plot ($1/k_{obs}$ versus $1/[S]$).

In the presence of inhibitor, biphasic time plots are obtained. The slope of the straight line going through the origin is called the early slope (k_e). Similarly, the second straight line gives the late slope (k_l). The early slope and the late slope were analyzed separately, according to the method of Kallia-Raftopoulos *et al.* (22). Following the same experimental procedure, we also determined the apparent equilibration rate constant (k_{eq}) of the reaction between complex C and inhibitor by assuming that this reaction proceeds toward equilibrium as a pseudo-first-order reaction.

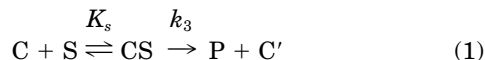
Detection of the Preincubation Effect

The preincubation effect with CAM or compounds **2–5** was detected through use of the spiramycin method (23). Briefly, complex C

either without or after preincubation (10 min, at 25°) with 5 K_i of inhibitor was exposed to 5×10^{-6} M spiramycin. The percentage (x') of the remaining active complex C, after washing of the cellulose nitrate filter to remove the excess antibiotics, was determined by titration with puromycin (2 mM, 2 min).

Results

Progress curve analysis. The reaction between the disc-adsorbed complex C (C) and excess puromycin (S) at 25° and in the presence of 10 mM Mg^{2+} proceeds as an irreversible pseudo-first-order reaction in which C is converted to C' (21).



As shown in Fig. 2 (top line), the progress curve of the reaction of eq. 1 (reaction 1) is a straight line at 200 μM puromycin. However, when reaction 1 occurs in the presence of analog 2, 3, 4, or 5, an early as well as a late phase can be seen clearly in the progress curves (Fig. 2). The deviation from linearity suggests a delay in the availability of complex C, which is engaged in reaction with inhibitor but is also needed in reaction 1. However, there was no substantial difference in the progress curves when the puromycin reaction was carried out after preincubation of complex C with the analogs (data not shown).

Analysis of the early slopes (k_e) by double-reciprocal plots and slope replots confirmed the results of a previous study (17) showing that analogs 2–4 behave as simple competitive inhibitors. The same kinetic examination was carried out for the analog 5. The results, shown in Fig. 3, are completely analogous. They show simple competitive inhibition. For comparison, the K_i values for analogs 2–5, together with the K_i value of CAM obtained in another study (8), are presented in Table 1.

When the inhibitory effect of analogs 2–4 is analyzed at the

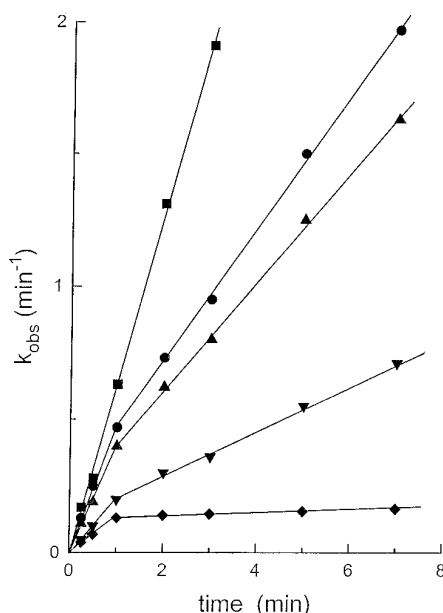


Fig. 2. First-order time plots for acetylphenylalanyl-puromycin formation in the absence or presence of several CAM analogs. Complex C reacts (■) with 200 μM puromycin (control) or with a solution containing 200 μM puromycin and 20 μM of (♦) 2, (▼) 3, (▲) 4, and (●) 5.

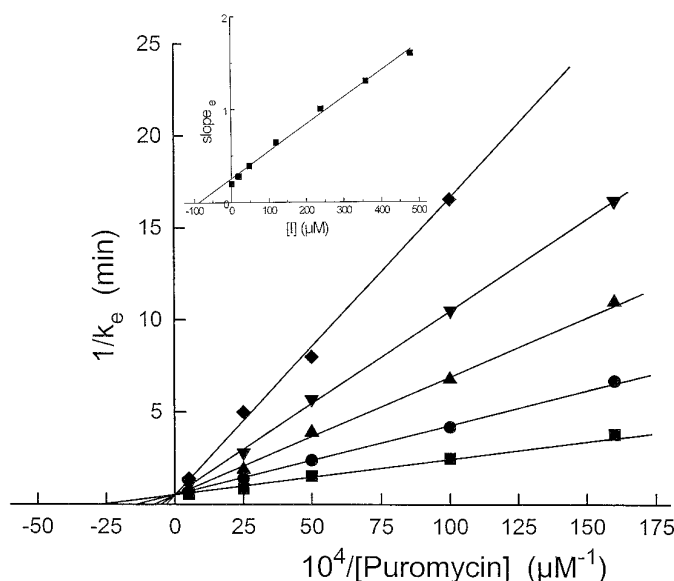


Fig. 3. Double-reciprocal plots ($1/k_e$ versus $1/[puromycin]$) for acetylphenylalanyl-puromycin formation in the presence or absence of analog 5. The data are obtained from the early slope of logarithmic time plots. The puromycin reaction is carried out (■) in the absence of analog 5 or in the following concentrations of analog 5: (●) 48 μM , (▲) 120 μM , (▼) 240 μM , and (♦) 480 μM . Inset, replot of the slopes of the double-reciprocal lines versus inhibitor concentration.

TABLE 1

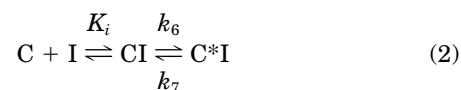
Equilibrium and kinetic constants derived from primary and secondary kinetic plots

The K_i and K'_i values are calculated from the negative intercept of the early and late slope replots, respectively. The k_6 and k_7 values are obtained from the sum ($k_6 + k_7$) and the ratio k_6/k_7 . The sum ($k_6 + k_7$) is obtained from the plateau of equilibration plots, whereas the ratio k_6/k_7 is calculated from the K'_i value of analogs via eq. 3. The k_{assoc} values are calculated from eq. 7.

Compound	K_i	K'_i	k_6/k_7	k_6	k_7	k_{assoc}
	μM			min^{-1}		$10^{-3} M^{-1} sec^{-1}$
1	0.7 ^a					
2	2.0	0.44	3.44	2.2	0.64	23.00
3	5.8	2.25	1.58	2.0	1.20	9.00
4	20.0	7.00	1.86	2.3	1.25	2.90
5	90.0	25.00	2.60	2.5	0.96	0.64

^a Data from Ref. 8.

late phase of the time plots (late slope, k_l analysis), the type of inhibition is, again, simple competitive. Furthermore, the linear slope replots meet the vertical axis at the point corresponding to the slope of the double-reciprocal plot of the control. Such a plot for analog 2 is given in Fig. 4. This observation strongly supports that the reaction between complex C and each of analogs 2–4 is expressed by eq. 2.



where the second step represents a slow isomerization of CI to C^*I .

From the negative intercept of the late slope replots, a different inhibition constant (K'_i) can be determined. The values of K'_i are given in Table 1. The slow-onset type of inhibition (22, 24) predicts the relationship

$$K'_i = K_i \frac{k_7}{k_6 + k_7} \quad (3)$$

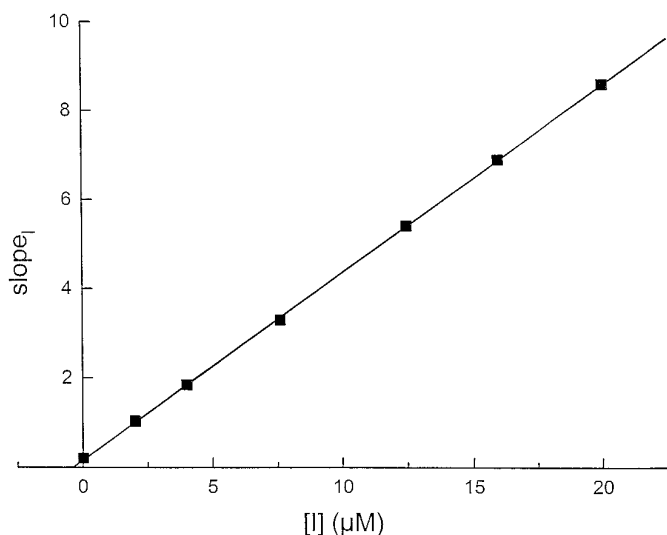


Fig. 4. Slope_i replots (slopes of double-reciprocal plots versus inhibitor concentration) for acetylphenylalanyl-puromycin formation in the presence of analog **2**.

Once both K_i and K'_i are calculated, the values of the ratio k_6/k_7 can be determined from eq. 3 and are given in Table 1.

Reaction 2 (eq. 2) *per se* may be considered a pseudo-first-order reaction going toward equilibrium with an apparent rate constant k_{eq} (22) given by eq. 4.

$$k_{eq} = k_7 + \frac{k_6[I]}{K_i + [I]} \quad (4)$$

Eq. 4 shows that when the concentration of I is much higher than K_i , the value of k_{eq} reaches a plateau, corresponding to the sum ($k_7 + k_6$). From this sum and the ratio k_6/k_7 , we can obtain approximate values for k_6 and k_7 (Table 1).

Late slope analysis for analog 5. Unexpectedly, the slope replot concerning analog **5** deviates from linearity (Fig. 5). Only over a narrow range of inhibitor concentrations ($[I] < 120 \mu\text{M}$), can we observe a transient phase of simple competitive inhibition (Fig. 5, *inset*). Consequently, only the

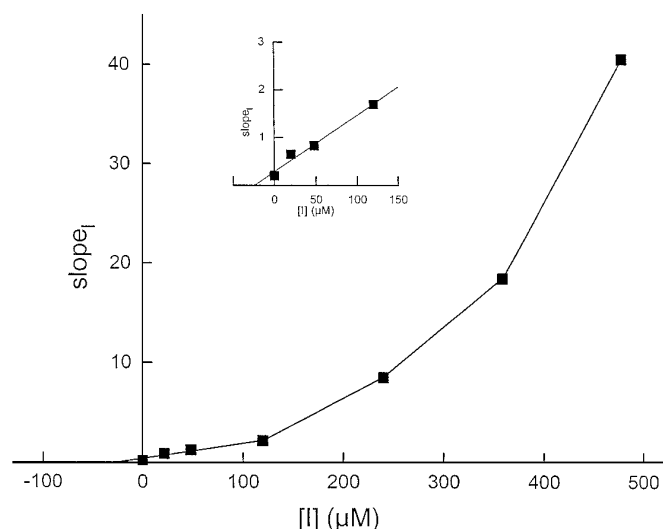


Fig. 5. Slope_i replot (slope of double-reciprocal plots versus inhibitor concentration) for acetylphenylalanyl-puromycin formation in the presence of analog **5**. *Inset*, detail for the transient phase of competitive inhibition at low concentrations of analog **5** ($[I] < 120 \mu\text{M}$).

initial kinetic behavior of inhibitor can be expressed by reactions 1 and 2. The values of K'_i , k_6/k_7 , k_6 , and k_7 calculated from experimental data of this transient phase are shown in Table 1. Increase in the concentration of analog **5** alters the type of inhibition to slope-parabolic competitive inhibition (25), characterized by a nonlinear slope replot. The parabolic curve of Fig. 5 indicates that there are more than one inhibitor binding sites. To evaluate the molecular order of analog **5** precipitation in puromycin reaction, the $\log[k_i/(k_{obs} - k_i)]$ values were calculated at each concentration of puromycin and plotted as a function of $\log[I]$ (26). Fig. 6 shows such a plot obtained for $400 \mu\text{M}$ puromycin. This plot is curved with limiting slopes of -1 at a very low $[I]$ and of -2 at a very high $[I]$.

A scheme that can adequately explain the kinetics of inhibition by analog **5** is shown in Fig. 7. According to this model, analog **5** exhibits a transient phase of competitive inhibition, followed by a slow isomerization of complex CI to C^*I and then by a second phase of competitive inhibition. This competitive inhibition during the second phase may be explained by tentatively accepting the formation of a species such as C^*I_2 , containing two molecules of analog **5**. The kinetic analysis of the late competitive phase (see Appendix) predicts that the late inhibition constant K''_i at various concentrations of inhibitor obeys the relationship:

$$K''_i = \frac{K_i k_7}{k_7 + k_6 \left(1 + \frac{[I]}{K_i^*}\right)} \quad (5)$$

The expression for K''_i can be rearranged to a linear form:

$$\frac{1}{K''_i} = \frac{1}{K_i} + \frac{k_6}{k_7 K_i K_i^*} [I] \quad (6)$$

Thus, if the reciprocal of the K''_i , determined from each double-reciprocal plot, is replotted versus the corresponding $[I]$, the replot will be a straight line with a slope equal to $k_6/k_7 K_i K_i^*$. With k_6 , k_7 , and K_i known, the K_i^* is estimated as $3.8 \pm 0.6 \times 10^{-5} \text{ M}$.

Reaction of spiramycin with complex C in the presence of CAM analogs. Spiramycin has been characterized as a slow-binding, slowly reversible inhibitor of peptide bond formation. It has been successfully applied to detect the preincubation effect exerted by CAM and lincomycin (23). By using the same method, we found that when a mixture of spiramycin with a CAM analog is used to replace spiramycin, a decrease in the apparent rate constant of inactivation of complex C (k_{in}) occurs. When complex C is preincubated with the CAM analog before the addition of spiramycin, a further decrease in k_{in} occurs. Fig. 8 represents the inactivation plots obtained with analog **2**. Similar results were obtained with analogs **3-5**. This effect (the preincubation effect) supports our proposal that the CAM analogs react with complex C as slow-binding inhibitors.

Discussion

In the current study, we examined the inhibition of peptide bond formation by several aminoacyl and peptidyl analogs of CAM in a model reaction in which peptidyl-tRNA is replaced by acetylphenylalanyl-tRNA and aminoacyl-tRNA is replaced by puromycin. The analogs interact with complex C with an apparent association rate constant of $<10^5 \text{ M}^{-1} \text{ sec}^{-1}$

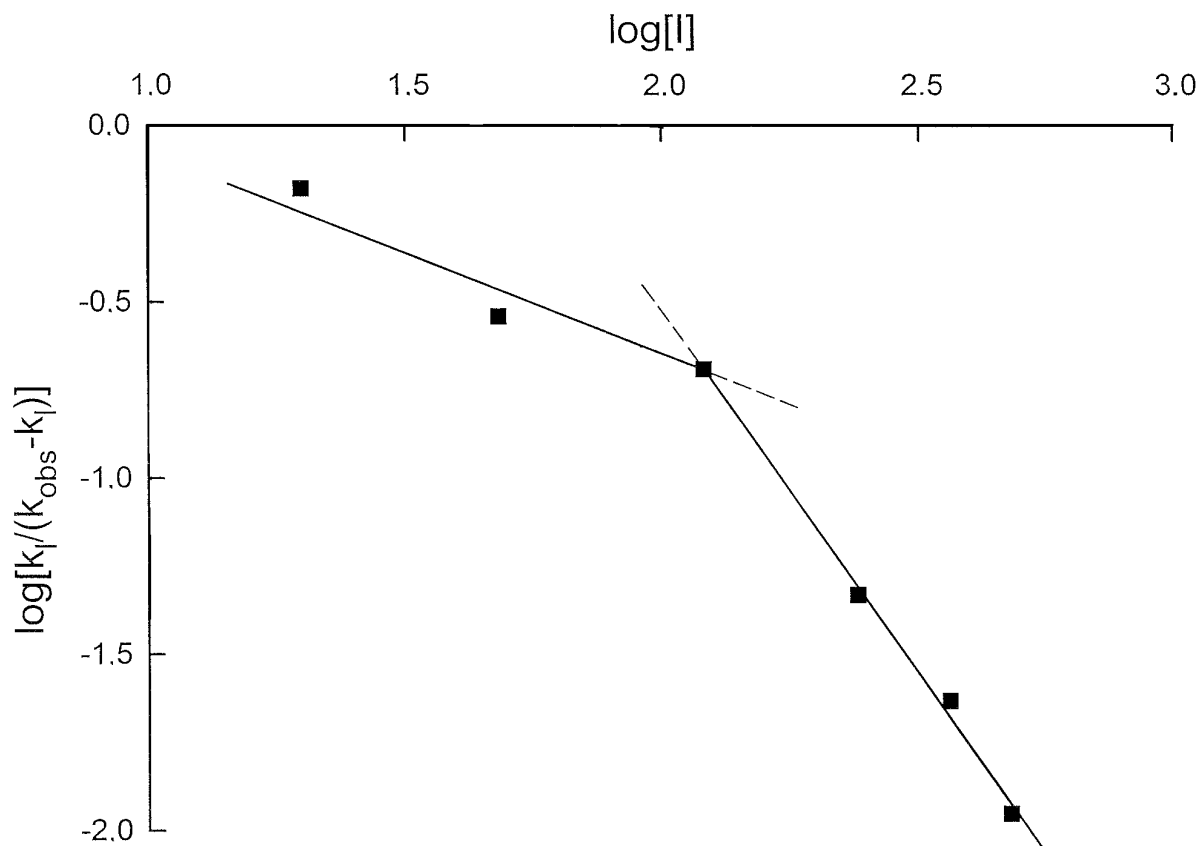


Fig. 6. Hill plot of inhibition of the puromycin reaction by analog **5**. Disc-adsorbed complex **C** is formed at 10 mM Mg^{2+} and then reacts at 25° with 400 μM puromycin in reaction buffer. The molecular interaction coefficient (n) of analog **5** is obtained from the slope of this plot. The k_i (in the presence of analog **5**) and k_{obs} (in the absence of analog **5**) values are calculated from the late phase of the corresponding logarithmic time plots.

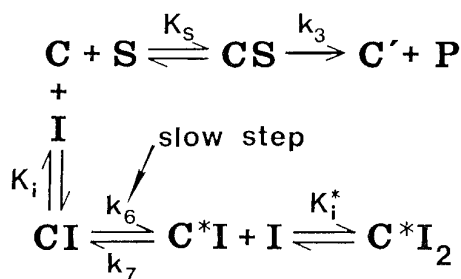


Fig. 7. Kinetic scheme proposed for the puromycin reaction in the presence of analog **5**. **C**, complex **C**; **I**, analog **5**; **C*****I**, isomerized complex **CI**; **S**, puromycin; **P**, acetylphenylalanyl-puromycin; **C**', ribosomal complex after its reaction with puromycin.

(Table 1). This value is $<10^6 \text{ M}^{-1} \text{ sec}^{-1}$, which is considered to be the upper limit for the characterization of a molecule as a slow-binding inhibitor (24). The biphasic progress curves suggest that the two-step model represented by eq. 2 is an adequate mechanism to explain the behavior of CAM analogs. Corroborative evidence comes from the hyperbolic shape of the equilibration plots (not shown) and particularly from the slope replots. The proposed mechanism suggests that the CAM analogs inhibit protein synthesis by binding initially to the ribosome in competition with puromycin. Subsequently, as a result of a conformational change, a slow isomerization occurs ($\text{CI} \rightleftharpoons \text{C}^*\text{I}$), after which the analogs continue to interfere with the binding of puromycin to the isomerized complex. It has been suggested that the binding of CAM to ribosomes induces conformational changes in the rRNA that

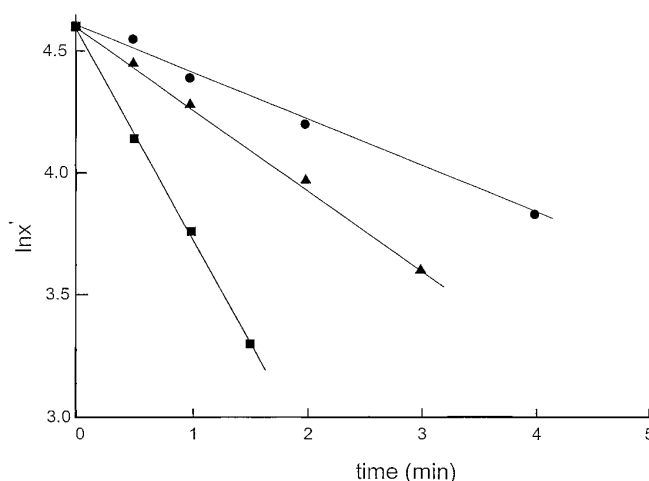


Fig. 8. First-order time plots for the inactivation of complex **C** by spiramycin when (■) spiramycin ($5 \times 10^{-6} \text{ M}$) alone is present or (▲) spiramycin ($5 \times 10^{-6} \text{ M}$) and analog **2** ($1 \times 10^{-5} \text{ M}$) are concomitantly present. In parallel, (●) complex **C** is preincubated with analog **2** at the same concentration as used previously, and then spiramycin ($5 \times 10^{-6} \text{ M}$) is added. The percentage (x') of the remaining active complex **C** is titrated by puromycin (2 mM, 2 min) after washing of cellulose nitrate filter to remove the excess antibiotics.

may be the basis for the inhibitory effect that CAM exerts on protein synthesis (4, 27–29). Probably during the reaction of eq. 2, the CAM analogs interact with the same sites of rRNA as does the parent compound. Thus, the analogs of CAM under investigation can be classified as members of the group

of slow-binding inhibitors. This group includes a number of important drugs and agrochemicals (24, 30).

For analog **5**, eq. 2 is extended by the binding of a second molecule of **5** to the isomerized complex C*I. This is consistent with the finding of other investigators that there are two sites on 70 S ribosomal particles for the binding of CAM (1–3, 5, 7, 28). It should be noticed that eq. 2 is a reduced form of the kinetic scheme of Fig. 7, when $K_i^* = \infty$. Our observations further support the idea that the competitive character of the CAM analogs, compared with the behavior of the parent compound (**8**), seems to be a result of an increased structural similarity of the analogs to the 3' terminus of aminoacyl-tRNA. Thus, the mixed noncompetitive type of inhibition observed in the case of CAM cannot be found even at high concentrations of the analogs or at the delayed phase of the puromycin reaction.

A common feature of slow-binding inhibitors is the “preincubation effect.” However, when the puromycin reaction was used to determine peptide bond formation, we failed to detect a preincubation effect with either the aminoacyl or the peptidyl analogs of CAM. This is in agreement with the fact that CAM also does not exhibit this effect (**8**). However, by exploiting the large difference between the k_3/K_s value ($73 \text{ M}^{-1} \text{ sec}^{-1}$) for the puromycin reaction and k_{assoc} ($3.3 \times 10^4 \text{ M}^{-1} \text{ sec}^{-1}$) for the spiramycin reaction, we were able to reveal the preincubation effect for the CAM analogs (Fig. 8). This fact further supports the characterization of the analogs under examination as slow-binding inhibitors.

According to previous reports, the potency of aminoacyl and peptidyl analogs of CAM has been assigned solely on the basis of the inhibition constant K_i (17) or of the parameter IC_{50} (16). This approach was based on the assumption that the equilibria concerning the inhibitor are attained instantaneously before a product is formed. However, this is inconsistent with the type of inhibition described in the present kinetic analysis. The K_i value alone cannot represent the potency of inhibitors at the late phase of inhibition. It is obvious that some additional constants should be used for fully characterizing the potency of CAM analogs. We propose the use of the apparent association rate constant k_{assoc} for evaluating the potency because it represents the overall tendency of complex C for engagement in reaction 2 (23). Although, the order of analog potency (17) is not disturbed by using the k_{assoc} instead of K_i as a criterion of potency, the relative inhibitory strength is altered. Thus, on the basis of the current calculation, we could say that analog **2** is 8-fold more potent than **4** and 2.5-fold more potent than **3**. Furthermore, according to the proposed model, we can explain why the relative potency of analog **5** is altered as a function of [I]. In contrast to the remainder of the analogs, analog **5** is characterized by a k_{assoc} value that is a linear function of [I].

$$k_{\text{assoc}} = \frac{k_7 + k_6 \left(1 + \frac{[\text{I}]}{K_i^*} \right)}{K_i} \quad (7)$$

Consequently, at very high [I], the value of k_{assoc} abruptly increases, resulting in a stronger inhibition of peptide bond formation.

It is worth noting that the “amide bond,” characterizing many inhibitors of peptidyltransferase (31), remains intact in the analogs used in the current work. It is also interest-

ing that the inhibitory activity of the compounds under investigation, although moderate compared with the parent compound, is nevertheless evident during the puromycin reaction. Although it is difficult to relate the L-*p*-methoxyphenylalanine moiety in puromycin to the examined analogs, which have a d-configuration, the competitive character of their action implies structural similarities to the acceptor molecule. It is significant that the configuration of an aminoacyl residue does not substantially affect the inhibitory ability of the respective analogs of CAM (32). Therefore, the model of CAM action proposed by Bhuta *et al.* (10) could successfully be extended to explain the relative activity of analogs **3–5**. By orienting the *p*-nitrophenyl group of these compounds to the hydrophobic locus of A-site, the CONH sequence of amide bonds in puromycin and CAM analogs is in the opposite direction. Thus, they can be regarded as retro-inverso analogs. In comparison to the parent compound **1**, it is obvious that replacement of the chlorine atoms by one hydrogen and one amino group (analog **3**) decreases the activity of CAM. The introduction of a benzyl side chain at the carbon bearing the free amino group of **3** gives the L-phenylalanyl analog **4**, which is less active than analog **3**. The possibility exists that the effect may be a modest electronic steric perturbation of the *p*-nitrophenyl moiety by the bulky acyl group, which alters its binding ability to the hydrophobic locus of A-site. Replacement of the dichloroacetyl group of CAM with the more extended L-glycyl-phenylalanyl moiety produces analog **5**, which is much less active than analog **4**. Furthermore, it seems that the conformational changes of complex C, caused by the binding of analog **5**, can accommodate the binding of a second molecule of **5** to ribosome. This second equilibrium results in a further increase in the apparent rate constant of complex C inactivation.

However, the *p*-nitrophenyl group of CAM analogs may not always be confined to the hydrophobic locus of ribosomal A-site. In fact, under certain structural limitations, the analog molecule may be better projected into the puromycin binding area, orienting its CONH sequence in a direction parallel to the amide bond of puromycin. Such a model has been proposed by McFarlan and Vince (16) and explains well the relative high activity of analog **2**. In comparison to isomer analog **5**, the biological activity of analog **2** revealed that the critical feature that influences the biological activity of the analogs is not the electronic structure at the acylamino chain but rather the stereospecificity of this region that determines the receptor engagement.

Acknowledgments

We are grateful to Dr. D. Drinain for valuable discussions during the progress of this work and for the critical reading of the manuscript. We also thank Dr. D. Synetos for reviewing the manuscript.

Appendix

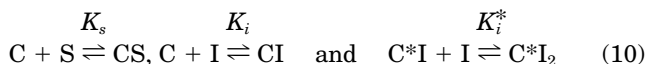
The rate of CS formation, corresponding to the kinetic scheme of Fig. 7, is given by the following equation:

$$\frac{d[\text{CS}]}{dt} = \frac{k_7[\text{S}][\text{C}_0 - \text{P}]}{K_s \left(1 + \frac{[\text{S}]}{K_s} + \frac{[\text{I}]}{K_i} \right)} - k[\text{CS}] \quad (8)$$

where

$$k = k_7 + \frac{k_3[S]/K_s + k_6[I]\left(1 + \frac{[I]}{K_i^*}\right)/K_i}{1 + \frac{[S]}{K_s} + \frac{[I]}{K_i}} \quad (9)$$

and C_0 represents the initial concentration of complex C. In deriving eq. 8, it is assumed that the equilibria

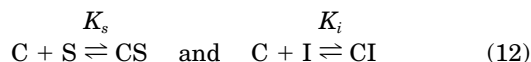


are established rapidly, whereas the isomerization of CI to C^*I ,



is established slowly.

Early competitive phase. As t approaches zero, there will be neither C^*I nor, consequently, C^*I_2 formation, but the equilibria



will have been established. Thus, eq. 8 is simplified to eq. 13:

$$\frac{d[CS]}{dt} = -\frac{k_3[S][CS]}{K_s\left(1 + \frac{[S]}{K_s} + \frac{[I]}{K_i}\right)} \quad (13)$$

Given that

$$\frac{dP}{dt} = k_3[CS], \quad (14)$$

eq. 13 can also be expressed as:

$$\frac{dP}{dt} = \frac{k_3[C_0 - P][S]}{K_s\left(1 + \frac{[S]}{K_s} + \frac{[I]}{K_i}\right)} \quad (15)$$

By integration of eq. 15, eq. 16 is obtained:

$$\ln \frac{[C_0]}{[C_0 - P]} = \ln \frac{100}{100 - x'} = k_e \cdot t = \frac{k_3[S]}{K_s\left(1 + \frac{[I]}{K_i}\right) + [S]} t \quad (16)$$

which is the integrated rate law for the initial stages of product formation in the presence of the inhibitor. From eq. 16, by setting $[I] = 0$, we obtain the rate law for reaction 1.

Late competitive phase. If we take into account that during the late phase of the logarithmic time plot the reaction $CI \rightleftharpoons C^*I$ has reached equilibrium, then $k_7[C^*I] = k_6[I]$. Under this assumption, eq. 8 is transformed to eq. 17:

$$[CS] = \frac{[C_0 - P][S]}{K_s\left(1 + \frac{[I]}{K_i^*}\right) + [S]} \quad (17)$$

where

$$K_i^* = \frac{K_i \times k_7}{k_7 + k_6\left(1 + \frac{[I]}{K_i^*}\right)} \quad (18)$$

By multiplying eq. 17 by k_3 , eq. 19 is obtained:

$$\frac{dP}{dt} = k_3[CS] = \frac{k_3[C_0 - P][S]}{K_s\left(1 + \frac{[I]}{K_i^*}\right) + [S]} \quad (19)$$

which by integration gives eq. 20:

$$\ln \frac{[C_0]}{[C_0 - P]} = \ln \frac{100}{100 - x'} = k_i \times t = \frac{k_3[S]}{K_s\left(1 + \frac{[I]}{K_i^*}\right) + [S]} t \quad (20)$$

References

1. Pongs, O. Chloramphenicol, in *Antibiotics V* (F. E. Hahn, ed.). Springer-Verlag, New York, 26–42 (1979).
2. Gale, E. F., E. Cundliffe, P. E. Reynolds, M. H. Richmond, and M. J. Waring. *The Molecular Basis of Antibiotic Action*. John Wiley & Sons, New York (1981).
3. Moazed, D., and H. F. Noller. Chloramphenicol, erythromycin, carbomycin and vanamycin B protect overlapping sites in the peptidyl transferase region of 23S ribosomal RNA. *Biochimie* **69**:879–884 (1987).
4. Marconi, R. T., J. S. Lodmell, and W. E. Hill. Identification of a rRNA/chloramphenicol interaction site within the peptidyltransferase center of the 50S subunit of the *Escherichia coli* ribosome. *J. Biol. Chem.* **265**:7894–7899 (1990).
5. Rodriguez-Fonseca, C., R. Amils, and R. A. Garrett. Fine structure of the peptidyl transferase centre on 23S-like rRNAs deduced from chemical probing of antibiotic-ribosome complexes. *J. Mol. Biol.* **247**:224–235 (1995).
6. O'Connor, M., and A. E. Dahlberg. The involvement of two distinct regions of 23S ribosomal RNA in tRNA selection. *J. Mol. Biol.* **254**:838–847 (1995).
7. Pestka, S. Studies on transfer ribonucleic acid-ribosome complexes. XIX. Effect of antibiotics on peptidyl puromycin synthesis on polyribosomes from *Escherichia coli*. *J. Biol. Chem.* **247**:4669–4678 (1972).
8. Drainas, D., D. L. Kalpaxis, and C. Coutsoygeorgopoulos. Inhibition of ribosomal peptidyltransferase by chloramphenicol: kinetic studies. *Eur. J. Biochem.* **164**:53–58 (1987).
9. Cheney, B. V. *Ab initio* calculations on large molecules using molecular fragments: structural correlations between natural substrate moieties and some antibiotic inhibitors of peptidyl transferase. *J. Med. Chem.* **17**:590–599 (1974).
10. Bhuta, P., H.-L. Chung, J.-S. Hwang, and J. Zemlicka. Analogues of chloramphenicol: circular dichroism spectra, inhibition of ribosomal peptidyltransferase, and possible mechanism of action. *J. Med. Chem.* **23**:1299–1305 (1980).
11. Rheinberger, H.-J., and K. H. Nierhaus. Partial release of AcPhe-Phe-tRNA from ribosomes during poly(U)-dependent poly (Phe) synthesis and the effects of chloramphenicol. *Eur. J. Biochem.* **193**:643–650 (1990).
12. Douthwaite, S. Functional interactions within 23S rRNA involving the peptidyltransferase center. *J. Bacteriol.* **174**:1333–1338 (1992).
13. Zemlicka, J., M. C. Fernandez-Moyano, M. Ariatti, G. E. Zurenko, J. E. Grady, and J. P. G. Ballesta. Hybrids of antibiotics inhibiting protein synthesis: synthesis and biological activity. *J. Med. Chem.* **36**:1239–1244 (1993).
14. Gu, Z., and P. S. Lovett. A gratuitous inducer of *cat-86*, ampicillin, inhibits bacterial peptidyl transferase. *J. Bacteriol.* **177**:3616–3618 (1995).
15. Coutsoygeorgopoulos, C., M. H. Fleysher, and J. T. Miller. Requirements for inhibition of peptide bond formation by analogs of chloramphenicol, in *Progress in Chemotherapy Proceedings of the 8th International Congress of Chemotherapy* (G. K. Daikos, ed.). Vol. 1. Hellenic Society of Chemotherapy, Athens, 417–420 (1974).
16. McFarlan, S. C., and R. Vince. Inhibition of peptidyltransferase and possible mode of action of a dipeptidyl chloramphenicol analog. *Biochem. Biophys. Res. Commun.* **122**:748–754 (1984).
17. Drainas, D., P. Mamos, and C. Coutsoygeorgopoulos. Aminoacyl analogs of chloramphenicol: examination of the kinetics of inhibition of peptide bond formation. *J. Med. Chem.* **36**:3542–3545 (1993).
18. Mamos, P., C. Sanida, and K. Barlos. Preparation of N-tritylamino acids from N-trimethylsilylamino acid trimethylsilyl esters. *Leibigs Ann. Chem.* 1083–1084 (1988).
19. Barlos, K., D. Papaioannou, and D. Theodoropoulos. Preparation and properties of N^a-tritylamino acid 1-hydroxybenzotriazole esters. *Int. J. Peptide Protein Res.* **23**:300–305 (1984).

20. Anderson, G. W., J. E. Zimmerman, and F. M. Callahan. The use of esters of N-hydroxysuccinimide in peptide synthesis. *J. Am. Chem. Soc.* **86**:1839–1842 (1964).
21. Kalpaxis, D. L., D. A. Theocharis, and C. Coutsogeorgopoulos. Kinetic studies on ribosomal peptidyltransferase: the behaviour of the inhibitor blasticidin S. *Eur. J. Biochem.* **154**:267–271 (1986).
22. Kallia-Raftopoulos, S., D. L. Kalpaxis, and C. Coutsogeorgopoulos. Slow-onset inhibition of ribosomal peptidyltransferase by lincomycin. *Arch. Biochem. Biophys.* **298**:332–339 (1992).
23. Dinos, G., D. Synetos, and C. Coutsogeorgopoulos. Interaction between the antibiotic spiramycin and a ribosomal complex active in peptide bond formation. *Biochemistry* **32**:10638–10647 (1993).
24. Morrison, J. F., and C. T. Walsh. The behavior and significance of slow-binding enzyme inhibitors. *Adv. Enzymol. Relat. Areas Mol. Biol.* **61**:201–301 (1988).
25. Segel, I. H. *Enzyme Kinetics*. John Wiley & Sons, New York (1975).
26. Kalpaxis, D. L., and D. Drainas. Inhibitory effect of spermine on ribosomal peptidyltransferase. *Arch. Biochem. Biophys.* **300**:629–634 (1993).
27. Langlois, R., C. R. Cantor, R. Vince, and S. Pestka. Interaction between the erythromycin and chloramphenicol binding sites on the *Escherichia coli* ribosome. *Biochemistry* **16**:2349–2356 (1977).
28. Grant, P. G., B. S. Cooperman, and W. A. Strycharz. On the mechanism of chloramphenicol-induced changes in the photoinduced affinity labeling of *Escherichia coli* ribosomes by puromycin: evidence for puromycin and chloramphenicol sites on the 30S subunit. *Biochemistry* **18**:2154–2160 (1979).
29. Porse, B. T., C. Rodriguez-Fonseca, I. Leviev, and R. A. Garrett. Antibiotic inhibition of the movement of tRNA substrates through a peptidyl transferase cavity. *Biochem. Cell Biol.* **73**:877–885 (1995).
30. Schloss, J. V. Significance of slow-binding enzyme inhibition and its relationship to reaction-intermediate analogues. *Accounts Chem. Res.* **21**:348–353 (1988).
31. Harris, R. J., and R. H. Symons. On the molecular mechanism of action of certain substrates and inhibitors of ribosomal peptidyl transferase. *Bioorg. Chem.* **2**:266–285 (1973).
32. Vince, R., R. G. Almquist, C. L. Ritter, and S. Daluge. Chloramphenicol binding site with analogues of chloramphenicol and puromycin. *Antimicrob. Agents Chemother.* **8**:439–443 (1975).

Send reprint requests to: Dr. D. L. Kalpaxis, Laboratory of Biochemistry, School of Medicine, University of Patras, GR-26110 Patras, Greece.
